# Downward migration of the zonal-mean circulation in the tropical atmosphere

**Kevin DallaSanta**[1,2], **Edwin P. Gerber**[1]

[1]Courant Institute of Mathematical Sciences, New York University, New York, New York, USA
[2]Now at NASA Goddard Institute for Space Studies, New York, New York, USA

**Key Points:**

- Zonally coherent, or annular, fluctuations capture a higher fraction of circulation variability in the tropics than they do in midlatitudes
- Annular anomalies in tropical geopotential height and zonal wind migrate from the tropopause to the surface over approximately 10 days
- Downward migration is associated with a pulsing of the overturning Hadley circulation on subseasonal time scales

Corresponding author: Kevin DallaSanta, kevin.dallasanta@nasa.gov

**Abstract**

The annular modes of the extratropical atmosphere have received much attention for quantifying variability of the jet streams and storm tracks, despite the fact that the midlatitude circulation itself does not vary uniformly with longitude. While tropical fluctuations in geopotential height have lower amplitude than in the extratropics, they exhibit stronger zonal coherence, or dynamical annularity. A simple index is developed to characterize zonal-mean anomalies of the tropical circulation. It reveals that anomalies in geopotential height and zonal wind migrate downward from the upper troposphere to the surface on a time scale of about 10 days. These features are distinguishable from known modes of tropical variability, the Madden–Julian Oscillation in particular. Evidence from reanalysis and idealized model experiments confirms that this downward migration is quite generic and driven by mechanically forced variations in the strength of the Hadley circulation on subseasonal time scales.

**Plain language summary:** Earth's atmosphere has certain recurring patterns which are "annular," spanning an entire latitude circle. Annular patterns have proven to be surprisingly useful for weather and climate prediction. However, in the tropics, annular patterns have not been studied. We show that annular variability in the tropics does exist, and it contains interesting features that may be useful for prediction. In particular, zonal anomalies in the circulation migrate downward from the tropopause (about 16 km) to the surface over 10 days. These features are also apparent in a relatively simple climate model, which helps direct further research.

## 1 Dynamical annularity of the atmospheric circulation

The annular modes of the extratropical circulation have received much attention for their predictive utility and dynamical insight (see Kushner, 2010, for an extensive review). They characterize atmospheric variability in a remarkable variety of contexts, from unforced intraseasonal variability (e.g., Thompson & Wallace, 1998; Feldstein, 2000) to forced responses associated with global warming (Thompson et al., 2000) or stratospheric ozone loss and recovery (Thompson et al., 2002). The designation "annular" refers to their zonally uniform structure, which characterizes an exchange of mass and momentum between the polar cap and midlatitudes (Thompson & Wallace, 2000), although their dynamics fundamentally depends on zonally asymmetric eddies (Hartmann & Lo, 1998).

From the time of their discovery, however, there has been much debate on the extent to which an annular mode, or midlatitude variability more generally, is actually annular. Deser et al. (2000) and Ambaum et al. (2001) observed that while variability of geopotential height becomes zonally uniform over the polar cap in a trivial sense, as the latitude circle approaches the scale of the deformation radius, variations in the midlatitudes are not at all zonally uniform.

More recently, Gerber & Thompson (2017) attributed the zonal structure of the annular mode patterns to the "statistical annularity" of the midlatitude circulation. The annularity of the pattern reflects the fact that the statistics of geopotential height variability are fairly uniform across longitudes, as opposed to the fluctuations themselves. They observed, however, that geopotential height variations in the tropics, while of weaker amplitude, exhibit far more zonal coherence.

The zonal coherence—or "dynamical annularity", to use the terminology of Gerber & Thompson (2017)—of geopotential height variability is quantified in Figure 1a. Here and throughout the study, data is taken from ERA–Interim reanalysis (Dee et al., 2011) from 1 January 1979 to 31 December 2017; JRA–55 (Kobayashi et al., 2015) reanalysis yields nearly identical results (not shown).

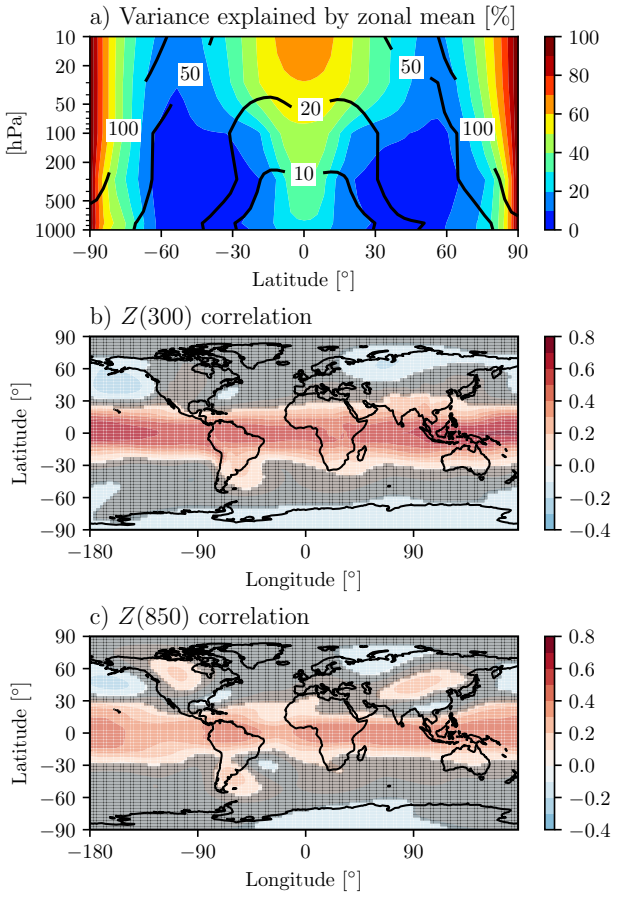


**Figure 1.** (a) The fraction of total variance associated with zonal mean anomalies in geopotential height (shaded), i.e., the power associated with wavenumber 0 in a zonal Fourier decomposition, normalized by the total power, and the RMS amplitude of the zonal mean flow (in meters; contoured). Unless specified otherwise, anomalies are defined as departures from a seasonally evolving climatology and high-pass filtered with a 1 year cutoff. (b) Correlation of 300 hPa geopotential height anomalies with our annular variability index $\overline{Z}(300\text{ hPa})$, described in the text. Hatching indicates regions where the correlation is not significantly different from 0 with 95% confidence, assuming a decorrelation time of 40 days to determine the degrees of freedom. (c) Same as (b), but showing the correlation of 850 hPa geopotential height anomalies with the $\overline{Z}(850\text{ hPa})$ index.

In the midlatitude troposphere—from 30 to 60° latitude in both hemispheres—less than 10% of variability is characterized by annular fluctuations. Near the poles, the geometry of the sphere naturally leads to a dominance of zonally coherent motion, but an additional maximum is observed in the tropics. Zonally coherent fluctuations of geopotential height characterize thus approximately a quarter of tropical variability at lower levels, the fraction increasing to almost a half at the tropopause. In this study, we investigate the structure of this zonally coherent variability in the tropical troposphere.

## 2 Downward migration of annular circulation anomalies in the tropics

We first establish a convenient index to quantify annular variability in the tropics: zonal-mean geopotential height at the equator, computed on a given pressure level and denoted $\overline{Z}(p)$. We find that this simple index correlates very highly with more complex metrics, such as the leading time series from Principal Component Analysis of tropical geopotential height (cf. Baldwin & Thompson, 2009). Since these more complex options involve selecting parameters, we proceed with the simplest option. The data is filtered by subtracting the seasonal cycle and subsequently high-pass filtered with a 1 year cutoff to remove trends and low-frequency variability such as El Niño–Southern Oscillation (ENSO). As we discuss below, filtering is not critical.

Figure 1b,c shows the structure of variability associated with $\overline{Z}(850)$ and $\overline{Z}(300)$. The indices characterize broad variations across the entire tropics, extending approximately 20 degrees from the equator, particularly in the Pacific sector which dominates the zonal mean. Broad correlation in geopotential reflects the weak rotation in the tropical atmosphere. In the weak temperature gradient limit Sobel et al. (2001), any localized heating or cooling of the atmosphere (e.g., by convection) is balanced by ascent or descent, thereby homogenizing the temperature, and hence geopotential height. The enhanced positive correlation in Figure 1b relative to Figure 1c reflects the increase in annular variability with height shown in Figure 1a.

To explore the vertical coupling between annular anomalies in geopotential height, Figure 2a shows the cross-correlation of $\overline{Z}(p)$ with $\overline{Z}(850)$. We begin with unfiltered data (from which only the annual cycle has been removed), but even in this raw reanalysis data, we see a downward migration of geopotential height anomalies from the upper troposphere to the surface on a time scale of about 10 days, followed by the hint of an opposite signed anomaly which also migrates downward. A comparable picture emerges if we choose other levels (e.g., 300 hPa) as our base level of correlation.

Low-frequency variability (primarily ENSO) and trends lead to significant redness in the unfiltered cross-correlations. The subseasonal time scale becomes more apparent after applying a highpass filtering with 1 year cutoff (Figure 2b). This conservative approach to removing the red background of the unfiltered cross-correlations still allows in more than half of the variance at a time scale of 1 year, and reveals more clearly a downward-migrating signal, anticorrelated with preceding and proceeding anomalies. In testing we find that the results are not sensitive to the cutoff provided it is short enough to remove ENSO.

Several approaches to significance testing underscore the robustness of this phenomenon. Hatching in Figure 2 indicates statistical significance assuming a decorrelation time scale of 40 days, a conservative approach intended to under-estimate the effective degrees of freedom. Subsetting the dataset by decades leads to similar results, as does employing composites instead of cross-correlations (not shown). Significance will furthermore be assessed dynamically by comparing observations with numerical models.

We first ask: is this downward migration simply the zonal mean manifestation of a known tropical mode of variability? Both the MJO (Andersen & Kuang, 2012) and ENSO (Seager et al., 2003) are known to exhibit zonally coherent variability. With respect to the latter, the high pass filtering in Figure 2b is one approach to removing the ENSO signal. (Alternatively, removing ENSO variability by regressing out the signal linearly correlated with the Niño 3.4 index yields a very similar result to Figure 2a). The highpass filter, however, will tend to amplify the relative importance of the MJO. To ensure the downward migration exists independently of the MJO, we repeated the analysis after regressing away variability linearly correlated with the principal components of the

Real-time Multivariate MJO (RMM) index (Wheeler & Hendon, 2004). Again, the results (not shown) are qualitatively identical with all MJO variability removed.

As an additional approach to answering this question, we consider a numerical model which explicitly lacks ENSO or MJO-related variability. The Model of an Idealized Moist Atmosphere (MiMA; Jucker & Gerber, 2017) is an idealized aquaplanet, and modifications to the original model have been made to incorporate realistic zonal asymmetries in the lower boundary; a later iteration of this configuration has been published in Garfinkel et al. (2020). There is explicitly no oceanic variability and the model does not capture the MJO. The model has no cloud feedbacks and only resolves the large-scale circulation, employing a simplified parameterization of tropical convection.

Despite these substantial simplifications, geopotential anomalies also migrate downward in MiMA, on comparable temporal and vertical scales (Figure 2c). If anything, the cross-correlations in MiMA are slightly reduced in magnitude, implying that the full physics of the actual atmosphere act to strengthen the downward migration, rather than weaken it. Furthermore, the horizontal structure of tropical geopotential height variations in the model is comparable to Figure 1b,c (not shown).

We have shown idealized moist aquaplanet integrations because this is perhaps the simplest configuration that can reproduce the phenomenon. When one removes the impact of moisture from the model, as in the idealized atmospheric model of Held & Suarez (1994), the downward migration of geopotential anomalies is not apparent, as we will address in Section 4. Dry dynamical cores are fully capable of capturing the annular modes (e.g., Gerber & Vallis, 2007), or the more recently discovered Baroclinic Annular Modes (Barnes & Thompson, 2014), but our results indicate that additional complexity is critical to capturing the annular variations of the tropics.

Although the MJO is not necessary for the downward-migrating signal in equatorial geopotential height, it does exhibit a similar signal. To quantify the MJO's signature on zonal-mean geopotential, we construct weighted composites of normalized geopotential anomalies at each level as a function of RMM phase (Wheeler & Hendon, 2004). Noting that 8 phases of the oscillation correspond to approximately 40 days, these composites show qualitatively similar downward migration on consistent time scales (Figure 2d). Thus in isolation an MJO event is sufficient, but not necessary, to achieve downward migration.

To get a sense of the actual variability, an example of downward migration for both positive and negative anomalies is shown in Figure 2e. Their vertical coherence and time scales are similar to the cross-correlated picture, and a lagged anticorrelation is apparent. These events and the cross-correlated average are reminiscent of the "dripping paint plots" of extratropical annular mode composites (Baldwin & Dunkerton, 2001), although the resemblance is superficial, as the dynamics of the two are quite distinct.

Downward migration in the Northern and Southern annular mode indices involves coupling between the tropospheric extratropical jet and the stratospheric polar vortex: a deceleration of the polar vortex is usually followed by a nearly barotropic response in the troposphere (Thompson & Wallace, 2000; Baldwin & Dunkerton, 2001). In the tropics, the downward migration is entirely within the troposphere. In addition, downward migration in the extratropical annular modes, while very robust, only appears in composite analysis and is not evident from simple cross-correlation, unlike the tropics.

Downward migration in the tropical circulation is also apparent in other meteorological variables, as shown in cross correlation of the zonal mean zonal wind with $\overline{Z}(850)$ in Figure 3a. Weakened trade winds migrate downward in association with anomalously high geopotential height, reflecting cyclostrophic balance. Conversely, strengthened trade wind anomalies migrate downward in concert with negative geopotential height anomalies. In the next section, we parse the structure of downward

migrating geopotential and zonal wind by cross-correlating with the key dynamical fields at play.

## 3 Mechanically forced variations in the Hadley Circulation

Geopotential height is the altitude of a given pressure surface of the atmosphere, and thus depends on both the surface pressure and the temperature of the atmosphere below. A pressure surface is elevated when the surface pressure increases; that is, when the local mass of the atmospheric column is increased, requiring one to ascend higher through the atmosphere to reach a given pressure. Similarly, a pressure surface is elevated if the atmosphere below it is warmer, and so less dense, again requiring a higher ascent to reach a given pressure. The downward migration of geopotential height anomalies shown in Figure 2 thus corresponds to a coordination, or phase locking, between temperature anomalies and surface pressure anomalies in the tropics.

Figure 3b,c show that anomalously high low-level geopotential (or surface pressure) is preceded by anomalously warm temperatures throughout the tropical troposphere, which lifts geopotential height at upper levels. Correlation between low-level geopotential and temperature reaches a maximum at a lead of 10 days ($-10$ on the horizontal axis), at which time surface pressure anomalies are uncorrelated: the atmosphere is warmest when surface pressure is neutral. The atmosphere cools as surface pressure anomalies build, with temperature anomalies vanishing at lag 0, just as surface pressure reaches a maximum. The atmosphere continues to cool, as surface pressure relaxes, reaching a maximum negative anomaly near a lag of 10 days (10 on the horizontal axis), maintaining quadrature with the surface pressure field.

Since the surface pressure indicates the total mass of the atmospheric column, downward migration in tropical geopotential can thus be described as a progression from *hot* to *heavy* (more mass) to *cold*. The cross-correlation is symmetric, by construction, but additional testing via composite analysis (not shown) reveals that this symmetry does hold between positive and negative anomalies: downward migration of negative geopotential height anomalies are associated with a cold–light–warm pattern.

This phase locking between temperature and surface pressure reflects a common dynamical origin: a pulsing of the Hadley circulation, illustrated in Figure 3d. On subseasonal time scales, the mean overturning circulation of the tropics is dominated by localized convection and associated downdrafts: hence only a weak, albeit statistically significant, zonal mean signal emerges from a noisy background. The anomalous warming of the tropics peaking at $-10$ days (Figure 3b) is associated with a suppression of convection (indicated by reduced precipitation, and consistent with an increase in gross moist stability) and a *weakening* in tropical upwelling (indicated by the positive correlation with the pressure velocity $\omega$ at 300 hPa). Upwelling is reduced at all tropospheric levels, suggesting an overall slowing of the overturning.

The anticorrelation between temperature and the upwelling velocity suggests that these anomalies are mechanically forced. Indeed, to generate kinetic energy thermodynamically, warm air must be associated with *increased* upwelling. The positive temperature anomalies (or equivalently, increase in moist stability) are consistent with a reduction in cooling driven by adiabatic expansion. Likewise, the reduction in upwelling throughout the tropical atmosphere is associated with a buildup of mass, such that surface pressure continues to increase until the overturning circulation begins to speed up again at lag 0.

The synchronous variation between $\omega$ and temperature would be expected on time scales where the radiative damping is sufficiently fast to bring the atmosphere in balance with mechanically forced upwelling anomalies. The effective radiative damping time scale of the tropical atmosphere at lower levels is sufficiently fast relative to the subseasonal

time scale of these oscillations (Jucker et al., 2013), but this is not the case at upper levels. Since precipitation is suppressed (Figure 3d) we conclude that latent heating is not responsible for warming at upper levels, but further work is needed to determine how the upper troposphere temperature anomalies remain synchronized.

## 4 Downward migration in idealized atmospheric models

As a probe of the downward migrating mechanism, we turn back to atmospheric model experiments. As shown in Figure 2c, downward migration was observed in MiMA which explicitly neglects clouds processes (see Jucker & Gerber, 2017, for further details). Thus cloud radiative feedbacks are unlikely to play a critical role in the mechanism. However, MiMA includes an idealized representation of land surfaces and oceanic heat transport to generate realistic stationary waves (as described in Garfinkel et al., 2020). Downward migration is nearly absent, however, in aquaplanet configurations in which all sources of zonal asymmetry in the lower boundary were removed. Hence stationary waves, or at least their impact on mean climatology and variability, are important.

Given the evidence in the previous section for a mechanical (momentum) forcing in the mechanism, we next probe the phenomenon in a dry atmospheric model. Here, radiative and moist processes are explicitly removed, and all thermodynamical processes are approximated by Newtonian relaxation to an equilibrium solstice temperature profile (Held & Suarez, 1994; Polvani & Kushner, 2002). The model nonetheless produces a fairly realistic Hadley Circulation, and vigorous midlatitude variability drives variations in tropical geopotential.

As seen in Figure 4a, the simplified physics of the dynamical core, however, are insufficient to generate a downward migration of geopotential anomalies. Use of an equilibrium equinox temperature profile, or integrations with large scale topography (Gerber & Polvani, 2009), not shown, exhibit a similar absence of downward migration. This indicates that momentum from the extratropics, associated with Rossby waves that break deep in the tropics, is insufficient to drive variations in the Hadley Cell that can phase lock the temperature and surface pressure variability.

While the moist and dry models share similar midlatitude variability, the moist model captures a more realistic representation of tropical variablity, in particular by simulating convectively coupled waves. The model is an extension of that explored by Frierson (2007) and shares a similar spectrum of tropical waves. To test whether the excitation of tropical waves are important, we introduce a simplistic tropical variability into the dry dynamical core through a prescribed temperature tendency.

Figure 4b shows the impact of artificially excited periodic variations in the tropical atmosphere, given by

$$\frac{\partial T}{\partial t} = \begin{cases} A\cos\left(2\pi\frac{t}{\tau}\right)\cos\left(\frac{\pi}{2}\frac{\phi}{\phi_0}\right) & |\phi| < \phi_0 \\ 0 & |\phi| > \phi_0 \end{cases} \tag{1}$$

where $A = 0.03$ K/day, $\tau = 32$ days, and $\phi_0 = 20$ degrees, chosen to mimic the features seen in reanalysis. The temperature perturbations are zonally and vertically uniform, since variations in the thermal damping time scale act to recover approximately the vertical structure seen in Figure 3a. When this periodic temperature forcing is applied in the dynamical core, downward migration re-emerges, reflecting the previous phase locking between temperature and surface pressure seen in reanalysis and MiMA. For these integrations, highpass filtering is applied at a cutoff of 90 days instead of 1 year, to compensate for its lack of seasonal cycle.

Experimentation with the vertical, meridional, and temporal variation of the temperature tendency indicates that the downward migration is fairly generic provided the time scale of forcing remains subseasonal, and the amplitude is strong enough to excite anomalies on the order of a few Kelvin. This suggests that tropically forced variability, associated with convectively coupled waves, may play a crucial role in the mechanism.

## 5 Summary

Annular variations in geopotential height capture a higher fraction of the natural variability in the tropical atmosphere as compared to the midlatitudes. We constructed a simple index to characterize the annular variability of the tropics: zonal-mean geopotential at the equator. The index tracks broad variations of the height fields at each level, extending approximately 20 degrees in latitude into both hemispheres. Cross-correlation between levels reveals downward-migrating circulation anomalies on intraseasonal time scales. Positive geopotential height anomalies, associated with decreased trade winds, migrate from the tropopause to the surface on a time scale of approximately 10 days. Likewise, enhanced trade winds migrate downward with negative geopotential height anomalies.

While the Madden–Julian Oscillation (MJO) is associated with a similar zonal mean signature, we find that these downward migration circulation anomalies are more generic. They reflect a phase locking of temperature and surface pressure anomalies associated with variations in the overturning circulation on intraseasonal time scales. Anticorrelation between the vertical velocity and temperature suggests that these variations are mechanically driven. Simulations with idealized atmospheric models attest to the generic nature of these downward migrating anomalies, but indicate that the mechanism depends on the presence of tropical variability. Future work intends to explore the mechanism in greater detail, and discuss the predictability of these oscillations.

**Acknowledgments**

We thank Olivier Pauluis and David Thompson for helpful discussion and feedback on earlier versions of this manuscript. This research was supported by the NSF through grant AGS-1852727 to New York University. KD also acknowledges support from the NASA Postdoctoral Program at the Goddard Institute for Space Studies.

## References

Ambaum, M. H., Hoskins, B. J., & Stephenson, D. B. (2001). Arctic Oscillation or North Atlantic Oscillation? *Journal of Climate*, *14*(16), 3495–3507.

Andersen, J. A., & Kuang, Z. (2012). Moist static energy budget of MJO-like disturbances in the atmosphere of a zonally symmetric aquaplanet. *Journal of Climate*, *25*(8), 2782–2804.

Baldwin, M. P., & Dunkerton, T. J. (2001). Stratospheric Harbingers of Anomalous Weather Regimes. *Science*, *294*(5542), 581–584.

Baldwin, M. P., & Thompson, D. W. (2009). A critical comparison of stratosphere–troposphere coupling indices. *Quarterly Journal of the Royal Meteorological Society*, *135*(644), 1661–1672.

Barnes, E. A., & Thompson, D. W. (2014). Comparing the roles of barotropic versus baroclinic feedbacks in the atmospheres response to mechanical forcing. *Journal of the Atmospheric Sciences*, *71*(1), 177–194.

Dee, D. P., Uppala, S. M., Simmons, A. J., Berrisford, P., Poli, P., Kobayashi, S., ... Dee, D. P. (2011). The ERA-Interim reanalysis: configuration and performance of the data assimilation system. *Q. J. R. Meteorol. Soc.*, *137*, 553–597.

Deser, C., Walsh, J. E., & Timlin, M. S. (2000). Arctic sea ice variability in the context of recent atmospheric circulation trends. *Journal of Climate*, *13*(3), 617–633.

Feldstein, S. B. (2000). The timescale, power spectra, and climate noise properties of teleconnection patterns. *Journal of Climate*, *13*(24), 4430–4440.

Frierson, D. M. (2007). Convectively coupled kelvin waves in an idealized moist general circulation model. *Journal of the atmospheric sciences*, *64*(6), 2076–2090.

Garfinkel, C. I., White, I., Gerber, E. P., Jucker, M., & Erez, M. (2020). The building blocks of northern hemisphere wintertime stationary waves. *Journal of Climate*(2020).

Gerber, E. P., & Polvani, L. M. (2009). Stratosphere–Troposphere Coupling in a Relatively Simple AGCM: The Importance of Stratospheric Variability. *J. Clim.*, *22*(8), 1920–1933.

Gerber, E. P., & Thompson, D. W. J. (2017). What Makes an Annular Mode Annular? *Journal of the Atmospheric Sciences*, *74*(2), 317–332.

Gerber, E. P., & Vallis, G. K. (2007). EddyZonal Flow Interactions and the Persistence of the Zonal Index. *J. Atmos. Sci.*, *64*(9), 3296–3311.

Hartmann, D. L., & Lo, F. (1998). Wave-driven zonal flow vacillation in the southern hemisphere. *Journal of the Atmospheric Sciences*, *55*(8), 1303–1315.

Held, I. M., & Suarez, M. J. (1994). A Proposal for the Intercomparison of the Dynamical Cores of Atmospheric General Circulation Models. *Bull. Am. Meteorol. Soc.*, *75*(10), 1825–1830.

Jucker, M., Fueglistaler, S., & Vallis, G. (2013). Maintenance of the stratospheric structure in an idealized general circulation model. *Journal of the atmospheric sciences*, *70*(11), 3341–3358.

Jucker, M., & Gerber, E. P. (2017). Untangling the annual cycle of the tropical tropopause layer with an idealized moist model. *J. Clim.*, *30*(18), 7339–7358.

Kobayashi, S., Ota, Y., Harada, Y., Ebita, A., Moriya, M., Onoda, H., ... Kiyotoshi, T. (2015). The JRA-55 reanalysis: General specifications and basic characteristics. *Journal of the Meteorological Society of Japan*, *93*(1), 5–48.

Kushner, P. J. (2010). Annular modes of the troposphere and stratosphere. *Geophysical Monograph Series*, *190*(1), 59–91.

Polvani, L. M., & Kushner, P. J. (2002). Tropospheric response to stratospheric perturbations in a relatively simple general circulation model. *Geophys. Res. Lett.*, *29*(7), 1114.

Seager, R., Harnik, N., Kushnir, Y., Robinson, W., & Miller, J. (2003). Mechanisms of hemispherically symmetric climate variability. *Journal of Climate*, *16*(18), 2960–2978.

Sobel, A. H., Nilsson, J., & Polvani, L. M. (2001). The Weak Temperature Gradient Approximation and Balanced Tropical Moisture Waves. *Journal of the Atmospheric Sciences*, *58*(23), 3650–3665.

Thompson, D. W. J., Solomon, S., & Hill, L. (2002). Interpretation of Recent Southern Hemisphere Climate Change. *Science*, *296*(5569), 895–899.

Thompson, D. W. J., & Wallace, J. M. (1998). The arctic oscillation signature in the wintertime geopotential height and temperature fields. *Geophysical research letters*, *25*(9), 1297–1300.

Thompson, D. W. J., & Wallace, J. M. (2000). Annular Mode in the Extratropical Circulation. Part I : Month-to-Month Variability. *J. Clim.*, *13*(1999), 1000–1016.

Thompson, D. W. J., Wallace, J. M., & Hegerl, G. C. (2000). Annular modes in the extratropical circulation. part ii: Trends. *Journal of climate*, *13*(5), 1018–1036.

Wheeler, M. C., & Hendon, H. H. (2004). An all-season real-time multivariate mjo index: Development of an index for monitoring and prediction. *Monthly weather review*, *132*(8), 1917–1932.

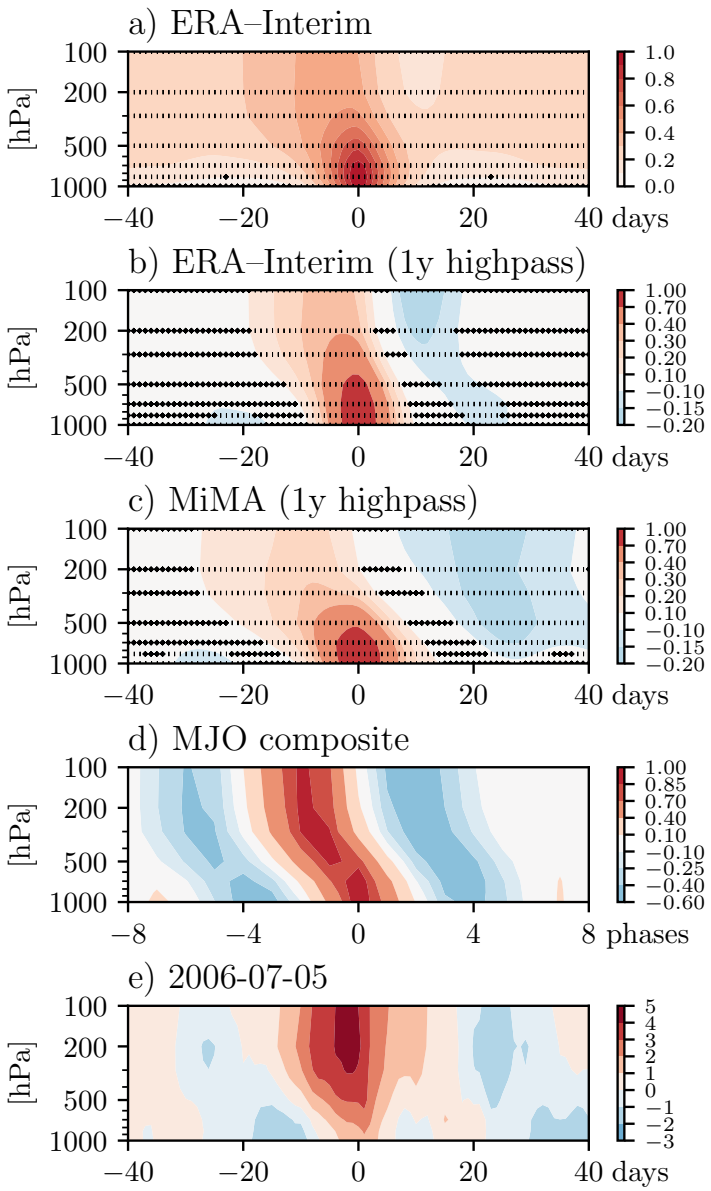


**Figure 2.** (a–d) Cross-correlation of $\overline{Z}(p)$ with $\overline{Z}(850)$. Data (a) from ERA–Interim unfiltered, (b) from ERA–Interim with a 1-year highpass filter, (c) from MiMA with a 1-year highpass filter, (d) composited by MJO RMM phase (amplitude-weighted; see text for details). (e) ERA–Interim $\overline{Z}(p)$ with a 1-year highpass filter, normalized to have unit variance, centered around July 5, 2006. In (a–c), hatching indicates inability to reject the null hypothesis that the correlation is zero with 95% confidence, using a decorrelation time of 40 days.

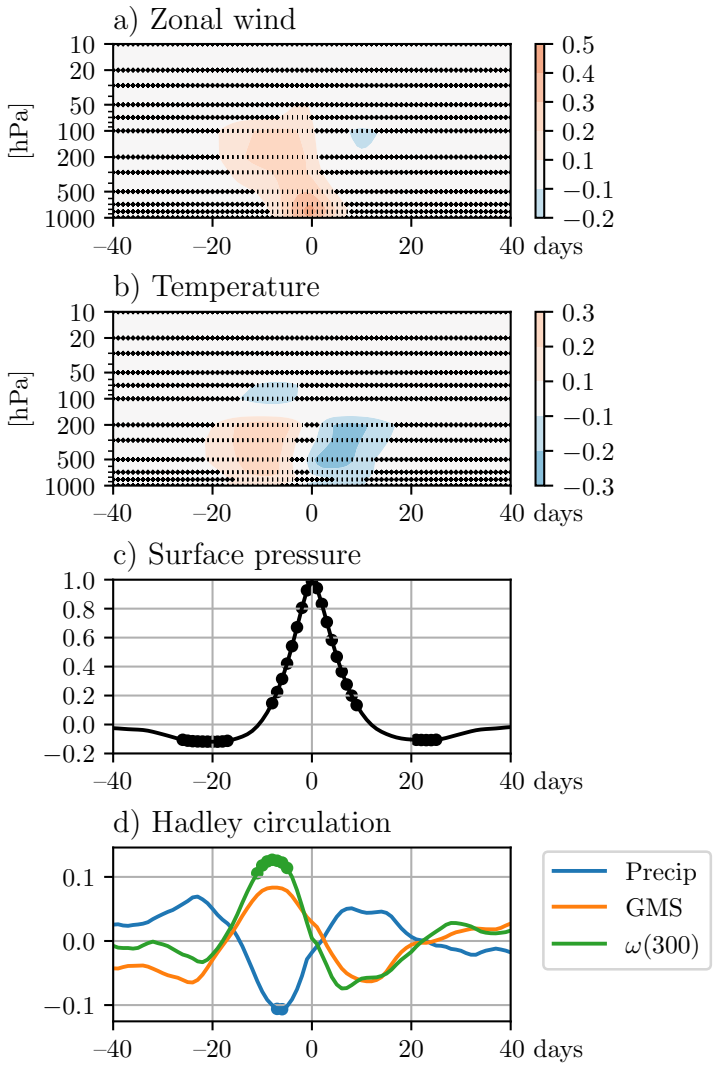


**Figure 3.** Cross-correlation of $\overline{Z}(850)$ with anomalous zonally averaged equatorial (a) temperature, (b) zonal wind, (c) surface pressure $p_s$, and (d) Hadley circulation metrics. In (d), the Hadley circulation is characterized by precipitation rate, gross moist stability (GMS; moist static energy at 850 hPa minus 200 hPa), and vertical velocity $\omega$ at 300 hPa. Data from ERA–Interim is, as before, deaseasonalized and 1-year highpass filtered. Hatching (a,b) and missing dots (c,d) indicate inability to reject the null hypothesis at 95% confidence, using a decorrelation time of 40 days.

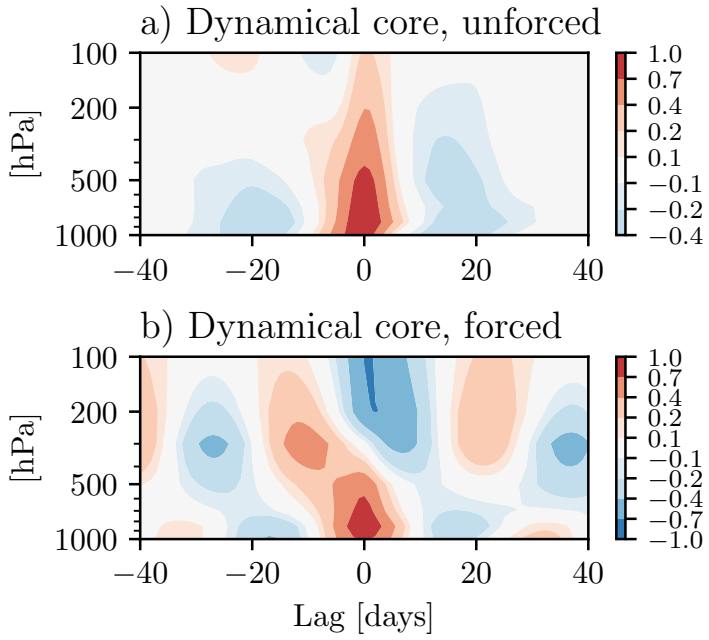


**Figure 4.** Cross-correlation of $\overline{Z}(p)$ with $\overline{Z}(850)$ in a dry dynamical core with Held & Suarez (1994) relaxation physics in (a) a control integration and (b) forced with the temperature tendency described in equation (1). Here the 1-year highpass filter is replaced by a 90-day bandpass filter, to compensate for the lack of seasonal cycle in the model.